

Anisotropic, Fermi-Surface-Induced Variation in  $T_c$  in  $MgB_2$  Alloys

Prabhakar P. Singh

Department of Physics, Indian Institute of Technology, Powai, Mumbai- 400076, India  
(April 14, 2024)

Using coherent-potential to describe disorder, Gaspari-Gyor' approach to evaluate electron-phonon coupling, and Allen-Dynes equation to calculate  $T_c$ , we show that in  $Mg_{1-x}M_xB_2$  ( $M = Al, Li \text{ or } Zn$ ) alloys (i) the way  $T_c$  changes depends on the location of the added/modified  $k$ -resolved states on the Fermi surface and (ii) the variation of  $T_c$  as a function of concentration is dictated by the B pDOS. In addition, using full-potential calculations for  $MgB_4$ , we show that (i) at  $x = 0.5$  a superstructure can form in  $Mg_{1-x}Al_xB_2$  but not in  $Mg_{1-x}Li_xB_2$  or  $Mg_{1-x}Zn_xB_2$ , and (ii) B layer shifts towards the impurity layer, more for Al than for Li or Zn.

PACS numbers: 74.25.Jb, 74.70.Ad

Since the discovery of superconductivity in  $MgB_2$  [1] the experimental [16] and theoretical [7,16] efforts have greatly improved our understanding of the nature of interaction responsible for superconductivity (SC) in  $MgB_2$ : It has become clear that almost all facets of the phonon-mediated electron-electron interaction have a dramatic influence over the superconducting behavior of  $MgB_2$ : For example, the electron-phonon matrix elements change considerably as one moves away from the cylindrical Fermi sheets along to  $A$  [9,16], anharmonic effects [6,15] have to be included in the dynamical matrix [16], and finally  $k$ -dependent fully anisotropic Eliashberg equations have to be solved [16] for a complete and accurate description of the superconducting properties of  $MgB_2$ : Such a strong dependence of the superconducting properties of  $MgB_2$  on different aspects of the interaction has opened up the possibility of dramatically modifying its superconducting behavior by changing the interaction in various ways and thereby learning more about the interaction itself. Alloying  $MgB_2$  with various elements and then studying their SC properties offers such an opportunity.

There have been several studies of changes in the SC properties of  $MgB_2$  upon substitutions of various elements such as Be; Li; C; Al; Na; Zn; Zr; Fe; Co; Ni; and others [5,17-20]. The main effects of alloying are seen to be (i) a decrease in transition temperature,  $T_c$ , with increasing concentration of the alloying elements although the rate at which the  $T_c$  changes depends on the element being substituted, (ii) a slight increase in the  $T_c$  in case of Zn [19,20] substitution while for Si and Li the  $T_c$  remains essentially the same, (iii) persistence of superconductivity up to  $x = 0.7$  in  $Mg_{1-x}Al_xB_2$  [5,17], (iv) a change in crystal structure and the formation of a superstructure at  $x = 0.5$  in  $Mg_{1-x}Al_xB_2$  [17], and (v) a change in the lattice parameters  $a$  and  $c$ :

In an effort to understand the changes in the electronic structure and the superconducting properties of  $MgB_2$  alloys, we have carried out *ab initio* studies of  $Mg_{1-x}Al_xB_2$ ;  $Mg_{1-x}Li_xB_2$  and  $Mg_{1-x}Zn_xB_2$  al-

loys. We have used Korringa-Kohn-Rostoker coherent-potential approximation [21,22] in the atomic-sphere approximation (KKR-ASAP) method for taking into account the effects of disorder, Gaspari-Gyor' formalism [23] for calculating the electron-phonon coupling constant  $\lambda$ , and Allen-Dynes equation [24] for calculating  $T_c$  in  $Mg_{1-x}Al_xB_2$ ;  $Mg_{1-x}Li_xB_2$  and  $Mg_{1-x}Zn_xB_2$  alloys as a function of Al; Li and Zn concentrations, respectively. We have analyzed our results in terms of the changes in the spectral function [22] along to  $A$  evaluated at the Fermi energy,  $E_F$ , and the total density of states (DOS), in particular the changes in the B p contribution to the total DOS, as a function of concentration  $x$ .

For examining the possibility of superstructure formation at  $x = 0.5$ ; we have used ABINIT code [25], based on pseudopotentials and plane waves to optimize the cell parameters  $a$  and  $c$  as well as relax the cell-internal atomic positions of  $MgAlB_4$ ;  $MgLiB_4$  and  $MgZnB_4$  in  $P6_3mm$  structures. We have used these atomic positions to carry out a total energy comparison using KKR-ASAP between the ordered and the substitutionally disordered  $Mg_{1-x}Al_xB_2$ ;  $Mg_{1-x}Li_xB_2$  and  $Mg_{1-x}Zn_xB_2$  alloys at  $x = 0.5$ . Such an approach allows us to check the possibility of formation of a layered or a mixed superstructure at  $x = 0.5$  in these alloys. Before we describe our results, we outline some of the computational details.

The charge self-consistent electronic structure of  $Mg_{1-x}Al_xB_2$ ;  $Mg_{1-x}Li_xB_2$  and  $Mg_{1-x}Zn_xB_2$  alloys as a function of  $x$  has been calculated using the KKR-ASAP method. We have used the CPA rather than a rigid-band model because CPA has been found to reliably describe the effects of disorder in metallic alloys [21,22]. We parametrized the exchange-correlation potential as suggested by Perdew-Wang [26] within the generalized gradient approximation. The Brillouin zone (BZ) integration was carried out using 1215  $k$  points in the irreducible part of the BZ. For DOS and spectral function calculations, we added a small imaginary component of 1 mRy and 2 mRy, respectively, to the energy

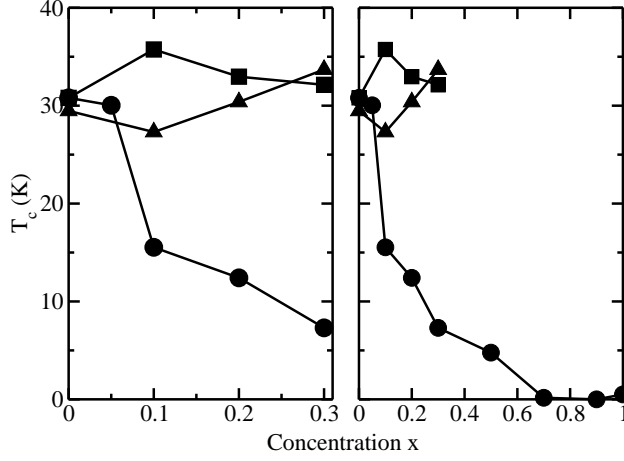


FIG. 1. The calculated variation of  $T_c$  as a function of concentration  $x$  in  $Mg_{1-x}Al_xB_2$ ,  $Mg_{1-x}Li_xB_2$  and  $Mg_{1-x}Zn_xB_2$  alloys.

and used 4900  $k$ -points in the irreducible part of the BZ. The lattice constants for  $Mg_{1-x}Al_xB_2$ ,  $Mg_{1-x}Li_xB_2$  and  $Mg_{1-x}Zn_xB_2$  alloys as a function of  $x$  were taken from experiments [17,19]. The Wigner-Seitz radii for Mg, Al and Zn were slightly larger than that of B. The sphere overlap which is crucial in ASA, was less than 10% and the maximum used was  $l_{max} = 3$ .

The electron-phonon coupling constant was calculated using Gaspari-Gyorffy [23] formalism with the charge self-consistent potentials of  $Mg_{1-x}Al_xB_2$ ,  $Mg_{1-x}Li_xB_2$  and  $Mg_{1-x}Zn_xB_2$  obtained with the KKR-ASA CPA method. Subsequently, the variation of  $T_c$  as a function of Al, Li and Zn concentrations was calculated using Allen-Dynes equation [24]. The average values of phonon frequencies  $\omega_{ln}$  for  $MgB_2$  and  $AlB_2$  were taken from Refs. [9,10] respectively. For intermediate concentrations, we took  $\omega_{ln}$  to be the concentration-weighted average of  $MgB_2$  and  $AlB_2$ . For  $Mg_{1-x}Li_xB_2$  and  $Mg_{1-x}Zn_xB_2$  we used the same value of  $\omega_{ln}$  as that for  $MgB_2$ .

The structural relaxation of  $MgAlB_4$ ,  $MgLiB_4$  and  $MgZnB_4$  was carried out by the molecular dynamics program ABINIT with Broyden-Fletcher-Goldfarb-Shanno minimization technique [25] using Troullier-Martins pseudopotentials [27], 512 Monkhorst-Pack [28]  $k$ -points and Teter parameterization [25] for exchange-correlation. The kinetic energy cutoff for the plane waves was 110 Ry.

Based on our calculations, described below, we find that in  $Mg_{1-x}Al_xB_2$ ,  $Mg_{1-x}Li_xB_2$  and  $Mg_{1-x}Zn_xB_2$  alloys (i) the way  $T_c$  changes depends on the location of the added/modified  $k$ -resolved states on the Fermi surface, (ii) the variation of  $T_c$  as a function of concentration

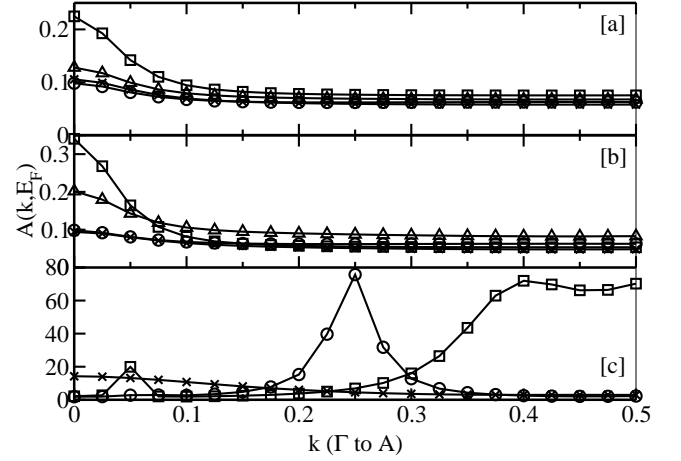


FIG. 2. The calculated spectral function along to  $A$ , evaluated at the Fermi energy, as a function of concentration  $x$  in  $Mg_{1-x}Al_xB_2$ ,  $Mg_{1-x}Li_xB_2$  and  $Mg_{1-x}Zn_xB_2$  alloys. Figures (a) and (b) correspond to  $x = 0.1$  and  $x = 0.3$ , respectively and the symbols open circle, open square,  $\times$  and open triangle correspond to  $MgB_2$ ,  $Mg_{1-x}Al_xB_2$ ,  $Mg_{1-x}Li_xB_2$  and  $Mg_{1-x}Zn_xB_2$  alloys respectively. In figure (c) the symbols open circle, open square and  $\times$  correspond to  $AlB_2$ ,  $Mg_{0.1}Al_{0.9}B_2$  and  $Mg_{0.4}Al_{0.6}B_2$ , respectively. For clarity, in figure (c) we have multiplied the spectral function of  $Mg_{0.4}Al_{0.6}B_2$  by 100.

is dictated by the Bp contribution to the total DOS, (iii) at  $x = 0.5$  a superstructure can form in  $Mg_{1-x}Al_xB_2$  but not in  $Mg_{1-x}Li_xB_2$  or  $Mg_{1-x}Zn_xB_2$ , and (iv) B layer shifts towards the impurity layer, more for Al than for Li or Zn:

The main results of our calculations are shown in Fig. 1, where we have plotted the variation in  $T_c$  of  $Mg_{1-x}Al_xB_2$ ,  $Mg_{1-x}Li_xB_2$  and  $Mg_{1-x}Zn_xB_2$  alloys as a function of concentration  $x$ . The calculations were carried out as described earlier with the same value of  $\omega_{ln} = 0.09$  for all the concentrations. The  $T_c$  for  $MgB_2$  is equal to 30.8 K; which is consistent with the results of other works [7,9,10] with similar approximations. The corresponding  $T_c$  is equal to 0.69. For  $0 < x < 0.3$ , the  $T_c$  increases slightly for  $Mg_{1-x}Li_xB_2$  and  $Mg_{1-x}Zn_xB_2$ , while it decreases substantially for  $Mg_{1-x}Al_xB_2$ ; as is found experimentally [5,17]. Note that for  $x = 0.1$ ; our calculation shows  $Mg_{1-x}Li_xB_2$  to have a  $T_c$  higher than that of  $Mg_{1-x}Zn_xB_2$  by about 7 K [18,20]. In Fig. 1 (right panel) we have shown the variation in  $T_c$  in  $Mg_{1-x}Al_xB_2$  alloys as a function of concentration for  $0 < x < 1$ : As a function of Al concentration, the  $T_c$  decrease rapidly from 30 K at  $x = 0.05$  to about 15 K at  $x = 0.1$ : The  $T_c$  decreases slowly between  $x = 0.4$  and  $x = 0.5$ : At  $x = 0.7$  the  $T_c$  vanishes and remains essen-

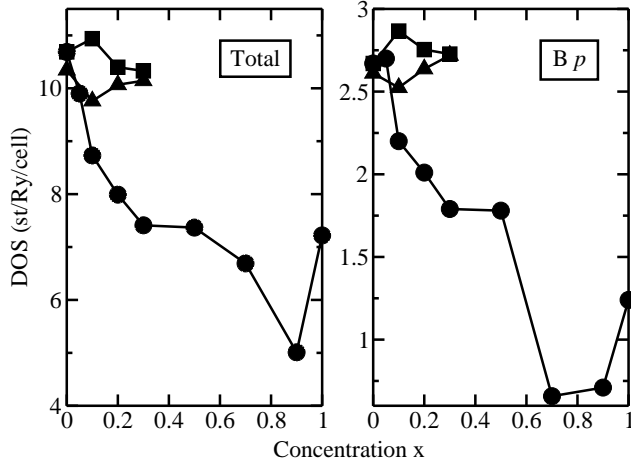


FIG. 3. The calculated total density of states at the Fermi energy (left panel) and the B p contribution to the total DOS (right panel) in  $Mg_{1-x}Al_xB_2$ ,  $Mg_{1-x}Li_xB_2$  and  $Mg_{1-x}Zn_xB_2$  alloys.

tially zero thereafter. The calculated variation in  $T_c$ , as shown in Fig. 1, is in very good qualitative agreement with the experiments [5].

In order to understand the variation of  $T_c$  in  $Mg_{1-x}Al_xB_2$ ,  $Mg_{1-x}Li_xB_2$  and  $Mg_{1-x}Zn_xB_2$  alloys as a function of concentration  $x$ , we have analyzed our results in terms of the spectral functions, the contribution of Boron p-electrons to the total DOS and the total DOS. In Fig. 2(a)–(c), we show the spectral functions along to A direction evaluated at  $E_F$  in  $Mg_{1-x}Al_xB_2$ ;  $Mg_{1-x}Li_xB_2$  and  $Mg_{1-x}Zn_xB_2$  alloys for  $x = 0.1$  (Fig. 2(a)),  $x = 0.3$  (Fig. 2(b)), and  $x = 0.6$ – $1.0$  (Fig. 2(c)). From Figs. 2(a)–(b) it is clear that the substitution of Al in  $MgB_2$  leads to creation of more new states along to A direction than the substitution of Zn or Li: Since the hole-like cylindrical Fermi sheet along to A contributes much more to the electron-phonon coupling [16], the creation of new electron states along to A direction weakens considerably the overall coupling constant; which, in turn, reduces the  $T_c$  more in  $Mg_{1-x}Al_xB_2$  than in either  $Mg_{1-x}Zn_xB_2$  or  $Mg_{1-x}Li_xB_2$ . Thus, in our opinion, the way  $T_c$  changes in  $MgB_2$  upon alloying depends dramatically on the location of the added/modified k-resolved states on the Fermi surface.

Having explained the differences in behavior of  $MgB_2$  upon alloying with Al, Li and Zn; we now try to understand the changes in their properties as a function of concentration  $x$ : In Fig. 3(a)–(b) we have shown the total DOS at  $E_F$  (Fig. 3(a)) and the B p contribution to the total DOS at  $E_F$  (Fig. 3(b)) in  $Mg_{1-x}Al_xB_2$ ;  $Mg_{1-x}Li_xB_2$  and  $Mg_{1-x}Zn_xB_2$  alloys as a function of concentration  $x$ : We find that as a function of concentra-

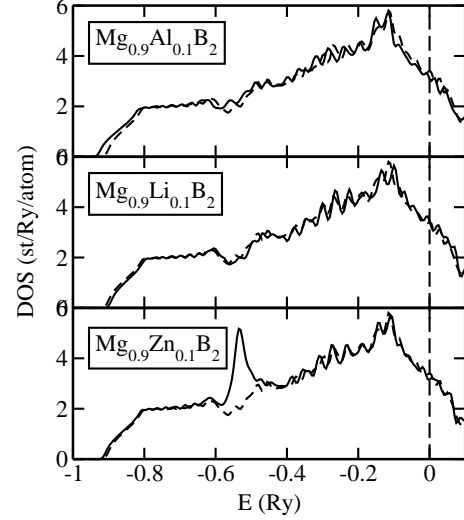


FIG. 4. The calculated total density of states (solid line) for  $Mg_{0.9}Al_{0.1}B_2$  (upper panel),  $Mg_{0.9}Li_{0.1}B_2$  (middle panel) and  $Mg_{0.9}Zn_{0.1}B_2$  (lower panel) alloys. For comparison the total DOS for  $MgB_2$  (dashed line) is also shown. The dashed vertical line indicates the Fermi energy.

tion, the variation in  $T_c$ , as shown in Fig. 1, follows closely the behavior of the total DOS at  $E_F$  and in particular the variation in B p contribution to the total DOS at  $E_F$ . It is also not surprising to see that the vanishing of superconductivity in  $Mg_{1-x}Al_xB_2$  at  $x = 0.7$  coincides with a very small B p contribution to the total DOS.

In Fig. 4(a)–(c) we show the total DOS of  $Mg_{1-x}Al_xB_2$ ,  $Mg_{1-x}Li_xB_2$  and  $Mg_{1-x}Zn_xB_2$  alloys, respectively, at  $x = 0.1$ : In the same plot we also show the total DOS of  $MgB_2$  obtained using the same approach. The overall downward (upward) movement of the total DOS in  $Mg_{0.9}Al_{0.1}B_2$  ( $Mg_{0.9}Li_{0.1}B_2$ ) with respect to that of  $MgB_2$  is due to the addition (removal) of electrons. In Fig. 4(c), the peak in the total DOS at around  $0.53$  Ry below  $E_F$  is due to the 3d states of Zn.

Finally, we discuss the possibility of superstructure formation at  $x = 0.5$ . In Table I we show the optimized cell parameters as well as the cell-internal relaxations for  $MgAlB_4$ ;  $MgL_iB_4$  and  $MgZnB_4$  calculated using the ABINIT program. We find that the Boron layer shifts significantly more towards Al layer in  $MgAlB_4$  than towards either Li or Zn layer in  $MgL_iB_4$  or  $MgZnB_4$ , respectively. The shift of B layer by  $0.24$  a.u.: towards Al layer in  $MgAlB_4$  compares well with the corresponding shift obtained in Ref. [29]. However, the shift of B layer towards Li and Zn layers in  $MgL_iB_4$  and  $MgZnB_4$  respectively implies that it is not simply due to the extra positive charge on the impurity layer, as suggested in Ref. [29] in the case of  $MgAlB_4$ : In Table I we have also listed the calculated ordering energy,  $E_{ord}$ ; which is the difference between the total energies of the

TABLE I. The calculated lattice constants  $a$  and  $c=a$ , the shift of the B layer along the  $c$ -axis towards the impurity layer, and the ordering energy  $E_{ord}$  at  $x = 0.5$ . The lattice constant  $a$  and the shift are in atomic units while  $E_{ord}$  is in m Ry=atom.

Alloy	$a$	$c=a$		$E_{ord}$
MgAlB <sub>4</sub>	5.799	2.242	0.24	-12.1
MgL iB <sub>4</sub>	5.685	2.287	0.04	+ 4.8
MgZnB <sub>4</sub>	5.789	2.254	0.08	+ 1.2

ordered MgAlB<sub>4</sub>, MgLiB<sub>4</sub> and MgZnB<sub>4</sub> and the corresponding disordered Mg<sub>0.5</sub>Al<sub>0.5</sub>B<sub>2</sub>; Mg<sub>0.5</sub>Li<sub>0.5</sub>B<sub>2</sub> and Mg<sub>0.5</sub>Zn<sub>0.5</sub>B<sub>2</sub> alloys, obtained using KKR-ASA CPA method. It clearly shows the possibility of formation of a superstructure in Mg<sub>0.5</sub>Al<sub>0.5</sub>B<sub>2</sub> because the fully-relaxed MgAlB<sub>4</sub> is lower in energy by 12 m Ry=atom in comparison to the disordered Mg<sub>0.5</sub>Al<sub>0.5</sub>B<sub>2</sub>. However, within the limitations of our approach, we find that Mg<sub>0.5</sub>Li<sub>0.5</sub>B<sub>2</sub> and Mg<sub>0.5</sub>Zn<sub>0.5</sub>B<sub>2</sub> are unlikely to form superstructures since  $E_{ord}$  is positive in these two cases. Our results also show that a structure made up of layers consisting of a random mixing of Mg and Al atoms and described by CPA, is higher in energy than a structure made up of alternate layers of Mg and Al atoms [29].

In conclusion, we have shown that in Mg<sub>1-x</sub>Al<sub>x</sub>B<sub>2</sub>; Mg<sub>1-x</sub>Li<sub>x</sub>B<sub>2</sub> and Mg<sub>1-x</sub>Zn<sub>x</sub>B<sub>2</sub> alloys (i) the way  $T_c$  changes depends on the location of the added/modified  $k$ -resolved states on the Fermi surface, (ii) the variation of  $T_c$  as a function of concentration is dictated by the B p contribution to the total DOS at  $E_F$ , (iii) at  $x = 0.5$  a superstructure can form in Mg<sub>1-x</sub>Al<sub>x</sub>B<sub>2</sub> but not in Mg<sub>1-x</sub>Li<sub>x</sub>B<sub>2</sub> or Mg<sub>1-x</sub>Zn<sub>x</sub>B<sub>2</sub>, and (iv) B layer shifts towards the impurity layer, more for Al than for Li or Zn:

[15] A. Liu et al, Phys. Rev. Lett. 87, 87005 (2001).  
[16] H. J. Choi et al, cond-mat/0111182 and cond-mat/0111183 (2001).  
[17] J. Y. Xiang et al, cond-mat/0104366 (2001).  
[18] Y. G. Zhang et al, Phys. C 361, 91 (2001).  
[19] S. M. Kazakov et al, cond-mat/0103350 (2001).  
[20] Y. Morimoto et al, cond-mat/0104568 (2001).  
[21] Prabhakar P. Singh and A. Gonis, Phys. Rev. B 49, 1642 (1994).  
[22] J. S. Faulkner, Prog. Mat. Sci. 27, 1 (1982); and references therein.  
[23] G. D. Gaspari and B. L. Gyor'y, Phys. Rev. Lett. 28, 801 (1972).  
[24] P. B. Allen and R. C. Dynes, Phys. Rev. B 12, 905 (1975).  
[25] See URL <http://www.pcpm.ucl.ac.be/abinit>.  
[26] J. P. Perdew and Y. Wang, Phys. Rev. B 45, 13244 (1992); J. Perdew et al, Phys. Rev. Lett. 77, 3865 (1996).  
[27] N. Troullier and J. L. Martins, Phys. Rev. B 43, 1993 (1991).  
[28] H. J. Monkhorst and J. D. Pack, Phys. Rev. B 13, 5188 (1976).  
[29] S. V. Barabash et al, cond-mat/0111392 (2001).

[1] J. Nagamatsu et al, Nature, 410, 63 (2001).  
[2] S. L. Bud'ko et al, Phys. Rev. Lett. 86, 1877 (2001).  
[3] D. G. Hinks et al, Nature 411, 457 (2001).  
[4] T. Takahashi et al, Phys. Rev. Lett. 86, 4915 (2001).  
[5] Cristina Buzea and Tsutomu Yamashita, cond-mat/0108265; and references therein.  
[6] T. Yildirim et al, Phys. Rev. Lett. 86, 5771 (2001).  
[7] J. Kortus et al, Phys. Rev. Lett. 86, 4656 (2001).  
[8] M. An and W. E. Pickett, Phys. Rev. Lett. 86, 4366 (2001).  
[9] Y. Kong et al, Phys. Rev. B 64, 020501 (2001).  
[10] K.-P. Bohnen et al, Phys. Rev. Lett. 86, 5771 (2001).  
[11] Prabhakar P. Singh Phys. Rev. Lett. 87, 087004 (2001).  
[12] N. I. Medvedeva et al, Phys. Rev. B 64, 020502 (2001).  
[13] G. Satta et al, Phys. Rev. B 64, 104507 (2001).  
[14] K. D. Belaschenko et al, Phys. Rev. B 64, 092503 (2001).